

1 **Lineage and stage-specific expressed *CYCD7;1* coordinates the single symmetric division that**
2 **creates stomatal guard cells**

3

4 Annika K. Weimer^{1,6}, Juliana L. Matos^{1,2,6}, Walter Dewitte^{3,4}, James A.H. Murray^{3,4}, Dominique C.
5 Bergmann^{1,5,*}

6 ¹ Department of Biology, Stanford University, Stanford, CA, USA

7 ² Present address: University of California Berkeley, Plant and Microbial Biology, Berkeley, CA, USA

8 ³ Cardiff School of Bioscience, Cardiff University, Wales, United Kingdom

9 ⁴ Institute of Biotechnology, University of Cambridge, United Kingdom

10 ⁵ Howard Hughes Medical Institute (HHMI), Stanford University, Stanford, CA, USA

11 ⁶ These authors contributed equally to this work.

12 * Author for correspondence: dbergmann@stanford.edu

13

14 **Running title:** CYCD7;1 triggers GMC divisions

15 **Keywords:** stomatal development, cell cycle, cyclin, cell division, differentiation, guard cell

16

17 **Summary statement:**

18 The core cell cycle component, CYCD7;1 requires stomatal transcription factors for its GMC-specific
19 expression; CYCD7;1 promotes the single symmetric division that ensures production of a 2-celled
20 stomatal complex.

21

22 **Abstract**

23 Plants, with cells fixed in place by rigid walls, often utilize spatial and temporally distinct cell division
24 programs to organize and maintain organs. This leads to the question of how developmental regulators
25 interact with the cell cycle machinery to link cell division events with particular developmental
26 trajectories. In *Arabidopsis* leaves, the development of stomata, two-celled epidermal valves that
27 mediate plant-atmosphere gas exchange, relies on a series of oriented stem-cell-like asymmetric
28 divisions followed by a single symmetric division. The stomatal lineage is embedded in a tissue whose
29 cells transition from proliferation to post-mitotic differentiation earlier, necessitating stomatal lineage-
30 specific factors to prolong competence to divide. We show that the D-type cyclin, CYCD7;1 is
31 specifically expressed just prior to the symmetric guard-cell forming division, and that it is limiting for

32 this division. Further, we find that CYCD7;1 is capable of promoting divisions in multiple contexts,
33 likely through RBR-dependent promotion of the G1/S transition, but that CYCD7;1 is regulated at the
34 transcriptional level by cell-type specific transcription factors that confine its expression to the
35 appropriate developmental window.

36

37 **Introduction**

38 Development of multicellular organisms requires the coordination and control of cell proliferation with
39 differentiation programs to generate distinct cell types, tissues and organs. Different cell lineages are
40 specified by sets of developmental regulators and display various cell proliferation dynamics, suggesting
41 that the cell cycle machinery might not always be comprised of the same components or controlled in
42 the same way. In *Arabidopsis*, the mature leaf epidermis contains pavement cells, trichomes and
43 stomata, three different functional cell types with their own developmental trajectories. Trichome
44 precursors are specified early and patterned via lateral inhibition networks (Schellmann et al., 2002), and
45 their maturation requires a shift from mitotic to endoreplication programs (Bramsiepe et al., 2010).
46 Pavement cells also endoreplicate as they acquire their lobed morphologies (Katagiri et al., 2016).

47

48 Stomata, pivotal for gas exchange between the plant and the environment, are derived from protodermal
49 cells in a process that requires them to first become self-renewing and multi-potent, but then to navigate
50 an ordered set of divisions and differentiation programs to create the mature stoma (Matos and
51 Bergmann, 2014). Stomatal development requires three essential, stage-specific, basic-helix loop-helix
52 (bHLH) transcription factors, SPEECHLESS (SPCH), MUTE and FAMA and their broadly expressed
53 heterodimer partners SCRM/ICE1 and SCRM2 (Kanaoka et al., 2008) (Fig 1A). SPCH drives
54 asymmetric cell divisions that initiate the lineage, creating meristemoids (M) that may undergo
55 continued self-renewing divisions. Plants lacking *SPCH* have no stomatal lineage. MUTE is essential to
56 terminate the asymmetric self-renewing divisions and to induce the differentiation of meristemoids into
57 guard mother cells (GMCs) (MacAlister et al., 2007; Pillitteri et al., 2007); loss of *MUTE* results in
58 excess meristemoids at the expense of GMCs (MacAlister et al., 2007; Pillitteri and Torii, 2007). FAMA
59 is required for the establishment of GCs but also to restrict GMCs to a single division. *fama* mutants
60 exhibit numerous rounds of symmetric and parallel GMC divisions without acquisition of terminal GC
61 identities (Matos et al., 2014; Ohashi-Ito and Bergmann, 2006). Plants bearing mutations in two R2R3

62 MYB transcription factor genes *FOUR LIPS (FLP)* and *MYB88* also exhibit *fama*-like GMC over-
63 proliferation phenotypes (Lai et al., 2005; Xie et al., 2010).

64

65 The varied trajectories of epidermal cells have been useful tools for dissecting cell cycle behaviors. The
66 components of the core cell cycle machinery are highly conserved among eukaryotes, though there has
67 been a large expansion of genes in plants (Harashima et al., 2013; Inzé and De Veylder, 2006). The plant
68 cell cycle is regulated by 5 main cyclin-dependent kinases (CDKs), CDKA;1, CDKB1;1, CDKB1;2,
69 CDKB2;1 and CDKB2;2. CDKs require cyclins (CYC) as binding partners for their kinase activity
70 toward downstream phosphorylation targets. Plants genomes encode much larger families of cyclin
71 genes than animals; for example, *Arabidopsis* encodes at least 32 cyclins (Vandepoele et al., 2002;
72 Wang et al., 2004) and it has been speculated that this expansion allows plants to specifically regulate
73 their postembryonic development (De Veylder et al., 2007; Harashima et al., 2013; Inzé and De Veylder,
74 2006). D-type cyclins as partners of CDKA;1 are critical for the G1/S cell cycle transition and
75 commitment to divide (Dewitte et al., 2007; Harbour and Dean, 2000; Riou-Khamlichi et al., 2000).
76 Eight out of ten plant CYCDs have an RBR1-binding motif (LxCxE) (Kono et al., 2007; Menges et al.,
77 2003). RBR1, the *Arabidopsis* homolog of the human tumor suppressor protein Retinoblastoma, is
78 crucial for the negative control of the cell cycle at G1/S transition (Desvoyes et al., 2006; Gutzat et al.,
79 2012; Nowack et al., 2012; Uemukai et al., 2005; Zhao et al., 2012). Phosphorylation of RBR1 by
80 CDKA;1/CYCD complexes inactivates its suppression of E2F transcription factors, allowing entry into
81 S phase and commitment to divide (Fig. 1B) (Harashima et al., 2013; Nakagami et al., 2002; Nowack et
82 al., 2012; Umen and Goodenough, 2001).

83

84 Here we show how the cell cycle and cell fate transition from GMCs to GCs is regulated by the
85 stomatal-lineage specific G1-S phase cell cycle regulator CYCD7;1. We demonstrate that CYCD7;1
86 activity is that of a typical D-type cyclin, but its expression window is narrowed by stomatal lineage
87 specific transcription factors. By examining how CYCD7;1 works with the core cell-cycle machinery
88 and with stomatal regulators, and by revealing the phenotypes upon loss and gain of *CYCD7;1* function,
89 we link a core cell-cycle regulator with a specific differentiation process and show how a formative
90 division is initiated but also restricted to allow “one and only one division” in GMCs to create a
91 physiologically functional valve structure from its two identical daughters.

92

93 **Results**

94 **CYCD7;1 is expressed prior to the last symmetric division in the stomatal lineage**

95 Among the 10 known D-type cyclins in *Arabidopsis*, *CYCD7;1* was uniquely enriched in transcriptional
96 profiles of Fluorescence Activated Cell Sorting (FACS) isolated cells of the late stomatal lineage
97 (Adrian et al., 2015). We confirmed this predicted expression in GMCs with transcriptional and
98 translational reporters (Fig. 1C-E) and observed that additional copies of *CYCD7;1-YFP* could force
99 ectopic divisions in GCs, suggesting that the protein could play a role in regulating this division (Fig.
100 1C, white arrowhead). A translational reporter, *pCYCD7;1:CYCD7;1-YFP*, was characterized previously
101 as peaking in GMCs (Adrian et al., 2015); however, the identity of *CYCD7;1* expressing cells was only
102 assessed by morphology. To refine the expression pattern, we co-expressed *pCYCD7;1:CYCD7;1-YFP*
103 with CFP reporters for SPCH, MUTE and FAMA (Fig. 1F-N). SPCH-CFP and *CYCD7;1-YFP*
104 expression appear to be mutually exclusive, suggesting that *CYCD7;1* is not expressed in meristemoids
105 (Fig. 1F-H). MUTE-CFP and *CYCD7;1-YFP* overlap in some cells, but we also see cells expressing
106 only MUTE or only *CYCD7;1*. Cells that only express MUTE had the morphology typical of
107 meristemoids, suggesting that MUTE is expressed before *CYCD7;1* (Fig. 1I-K). When compared to
108 FAMA expression, *CYCD7;1-YFP* appears to be expressed before FAMA-CFP in GMCs, briefly
109 together with FAMA in newly divided GCs, and then disappears before FAMA in GCs (Fig. 1L-N).
110 Thus, the expression of *CYCD7;1* in the stomatal lineage is temporally and spatially controlled and
111 starts after MUTE expression and finishes before FAMA expression (Fig. 1A).

112

113 We did not observe expression of *CYCD7;1-YFP* in any vegetative tissue from the seedling stage
114 through flowering (data not shown). In adult plants, *CYCD7;1-YFP* was expressed in pollen sperm cells
115 at anthesis, but not in the vegetative nucleus (Fig. S1). The expression of a D-type cyclin (typically
116 expressed at G1/S) is consistent with the observations that sperm cells undergo an extended S phase in
117 mature pollen grains (Friedman, 1999; Zhao et al., 2012).

118

119 Why does *CYCD7;1* have such a restricted expression pattern in the stomatal lineage? One possible
120 explanation is that *CYCD7;1* has a unique function in GMC divisions. A second possibility is that
121 *CYCD7;1* has a canonical role, i.e. it acts like other cyclins in promoting cell divisions, but it is
122 important to be able to tightly control deployment of that role in the stomatal lineage. To distinguish
123 between these models, we characterized plants missing or misexpressing *CYCD7;1*, tested relationships

124 between CYCD7;1 and other cell cycle regulators, and defined how *CYCD7;1* expression was
125 constrained by stomatal lineage transcription factors.

126

127 **Ectopic expression of CYCD7;1 triggers divisions while *cyclinD7;1* mutants decelerate GMC
128 divisions**

129 If CYCD7;1 has canonical CYCD activity, it should be able to promote cell divisions outside its normal
130 expression window. To test this, we expressed CYCD7;1 and CYCD7;1-YFP with the pan-epidermal
131 promoter, ML1 (Roeder et al., 2010). Ectopic expression of CYCD7;1 (YFP-tagged or untagged)
132 induced cell divisions of pavement cells in the leaf (Fig. 2A-C) indicating that CYCD7;1 can function as
133 a canonical D-type cyclin.

134

135 Next, we asked if mutations of *CYCD7;1* result in abnormal phenotypes. We obtained multiple alleles of
136 *CYCD7;1*: FLAG_369E02 (*cyclinD7;1-1* (Collins et al., 2012), FLAG_498H08 (*cyclinD7;1-2*), GK_496G06-
137 019628, SALK_068526 and SALK_068526 (Fig. S2A). We determined by qRT-PCR that *cyclinD7;1-1*
138 (FLAG_369E02) produced no transcript (Fig. S2B). On a whole plant level, we could not detect any
139 abnormalities in *cyclinD7;1-1* compared to wild type (Fig. S1C). Because CYCDs promote G1/S transitions
140 and CYCD7;1 is specifically expressed during the GMC divisions, we asked whether *cyclinD7;1-1* mutants
141 halt this transition by counting GCs in cotyledons. Mutants in *cyclinD7;1-1* do not display fewer GCs
142 compared to wild type 7 days after germination (dag) (Fig. S2D-F). However, at 4 dag, when cells in the
143 earlier stages of the stomatal lineage are abundant, *cyclinD7;1-1* cotyledons have more GMCs compared to
144 wild type cotyledons (Fig. 2D). Interestingly, the average size of *cyclinD7;1-1* GMCs is larger than wild
145 type (Fig. 2E). We confirmed that these GMC abundance and size phenotypes were present in plants
146 bearing a different allele of *CYCD7;1* (*cyclinD7;1-2*) (Fig. S2G, H). Plant cells are known to increase in
147 size during G1, so this phenotype suggests that CYCD7;1 hastens cell cycle progression in the GMC to
148 GC transition. Because *cyclinD7;1-1* is the null allele, we characterized its phenotypes in more detail. We
149 introgressed *pCDKB1;1:GUS*, which labels the transition from GMC to GCs (Boudolf et al., 2004), into
150 *cyclinD7;1-1* mutants. Compared to wild type, *cyclinD7;1-1* mutants show increased number of GUS-positive
151 cells suggesting that these cells remain longer in GMC fate before they divide into GCs (Fig. 2F-H). To
152 directly test this hypothesis, we labeled S phases with 5-ethynyl-2'-deoxyuridine (EdU) a thymidine
153 analogue readily incorporated during DNA replication (Fig. 2I, J). Strikingly, significantly fewer GMCs
154 in *cyclinD7;1-1* showed EdU labeling (indicating that they were in S phase during the EdU pulse)

155 compared to wild-type GMCs (Fig. 2K). Together these data suggest that CYCD7;1 is required for
156 GMCs to make a timely entry into S phase before their transition into GCs.

157

158 **CYCD7;1 interacts with RBR1**

159 Typically, CYCDs drive the G1/S transition through inactivation of RBR1, and RBR1 activity was
160 previously shown to be essential for repressing divisions in the stomatal lineage (Borghi et al., 2010;
161 Matos et al., 2014). If CYCD7;1 and RBR1 function together, we would expect them to be co-
162 expressed, to physically interact, and for there to be a phenotypic consequence of disrupting the
163 interaction. Indeed, CYCD7;1 and RBR1 were shown to physically interact in BIFC and Y2H assays,
164 dependent on the presence of the RBR1 binding motif LxCxE in CYCD7;1 (Matos et al., 2014). In
165 addition, CYCD7;1 and RBR1 are co-expressed in GMCs (Fig. 3A-C). To test whether this interaction is
166 functionally important, we took advantage of the fact that our translational reporter of CYCD7;1 triggers
167 extra cell divisions in GCs (Fig. 1C, Fig. 3 D,E). Approximately 24% of GCs have one and 18% have
168 two ectopic divisions in *pCYCD7;1:CYCD7;1-YFP* plants at 5 dag (Fig. 3G). If the RBR1 interaction is
169 important for CYCD7;1 function, then mutation of the RBR1 binding motif LxCxE into LxGxK in
170 CYCD7;1, should abrogate this division promoting activity. Strikingly, we found that
171 *pCYCD7;1:CYCD7;1^{LGK}-YFP* no longer triggers ectopic cell divisions in GCs (Fig. 3F,G). This effect
172 was not due to differences in expression levels between *CYCD7;1-YFP* and *CYCD7;1^{LGK}-YFP* (Fig
173 S1B). Production of ectopic cell divisions in GCs, therefore, depends on the RBR1 binding residues in
174 CYCD7;1.

175

176 **CYCD7;1 needs CDKB1 activity to drive ectopic divisions**

177 Cyclins bind to CDKs to ensure kinase activity and completion of cell division; undivided cells
178 expressing GC fate markers result from reduction or loss of CDK activity (e.g., hypomorphic *cdka;1*
179 mutants (Weimer et al., 2012), *cdkb1;1 cdkb1;2* double mutants (Xie et al., 2010) or dominant-negative
180 CDKB1;1-N161 (Boudolf et al., 2004)). To test whether CYCD7;1 required CDK activity to drive
181 divisions, we expressed CYCD7;1-YFP and CYCD7;1^{LGK}-YFP under the CYCD7;1 promoter in plants
182 bearing a dominant negative version of *CDKB1;1* (CDKB1;1-N161, Fig. 3H-J). Although we could see
183 expression of both CYCD7;1 markers in arrested GMCs, they could neither rescue the phenotype nor
184 trigger ectopic cell divisions (Fig. 3I-K). Thus CYCD7;1 requires CDKB1 activity either as a partner, or
185 downstream at the G2/M transition for completion of the division.

186 **CYCD7;1 expression domain is constrained by stomatal lineage transcription factors**

187 Our evidence points to CYCD7;1 acting like a canonical CYCD, therefore we turned our attention to
188 regulation of its highly restricted expression pattern. Three transcription factors are contemporaneously
189 expressed with CYCD7;1—MUTE, FAMA and FLP (Fig 1I-K)—but MUTE precedes CYCD7;1 while
190 the others persist longer. Given these patterns, we tested whether MUTE was necessary for CYCD7;1
191 expression. When *pCYCD7;1:CYCD7;1-YFP* was crossed into the *mute* mutant, we could observe the
192 typical *mute* phenotype of many small meristemoid-like cells that fail to differentiate into GMCs
193 (Pillitteri et al., 2007). In a few of these meristemoid-like cells, we detected weak CYCD7;1-YFP signal
194 (Fig. 4A,B). Fluorescence intensity measurements showed that CYCD7;1-YFP signals in *mute* are ~50%
195 reduced (Fig 4C-F) indicating that MUTE promotes CYCD7;1 expression, though it is not absolutely
196 essential for it. In none of these images did we observe any ectopic divisions of the meristemoid-like
197 cells.

198

199 CYCD7;1 appears to be repressed during FAMA’s expression peak. We therefore tested whether
200 FAMA, in its role as the master transcriptional regulator of stomatal division and differentiation, is a
201 direct regulator of CYCD7;1. In *fama* mutants GMCs divide repeatedly without attaining GC fate (Fig.
202 5A-E) and these “tumors” express CYCD7;1-YFP (Fig. 5B,C); although the reporter fades in older
203 leaves suggesting that CYCD7;1-YFP is also subject to posttranslational regulation (Fig. 5D,E). In the
204 *fama* tumors, *pCYCD7;1:CYCD7;1-YFP* drives ectopic divisions (Fig. 5B,D, white arrowheads), but the
205 *CYCD7;1^{LGK}* version that cannot bind RBR1, does not (Fig. 5C,E). To test whether FAMA might
206 directly regulate CYCD7;1, we extracted reads from a FAMA ChIP-seq experiment, performed under
207 similar conditions as in (Lau and Bergmann, 2015; Lau et al., 2014). As shown in Fig. 5F, it is clear that
208 FAMA is associated with the promoter region and gene body of *CYCD7;1*.

209

210 Along with FAMA, two partially redundant R2R3 MYB transcription factors, FOUR LIPS (FLP) and
211 MYB88, restrict GMC divisions. Previously, it was shown that FLP/MYB88 bind directly to the
212 *CDKB1;1* promoter and can repress *CDKB1;1* transcription (Lee et al., 2013; Vanneste et al., 2011; Xie
213 et al., 2010). *flp/myb88* mutants also display GMC overproliferation but, unlike *fama* mutants, some
214 differentiated GCs form (Lai et al., 2005; Xie et al., 2010), Fig. 4F,I). *CYCD7;1-YFP* (and *CYCD7;1^{LGK}-YFP*)
215 translational reporters are highly expressed in *flp/myb88*, and *CYCD7;1-YFP*, but not
216 *CYCD7;1^{LGK}-YFP*, induces ectopic divisions (Fig. 4 G,H,J,K).

217 The phenotypes of loss and gain of CYCD7;1 activity suggest that its narrow window of expression is
218 essential to guarantee a 2-celled stomatal complex. Using the *FAMA* promoter in wild type, thus driving
219 CYCD7;1 slightly later than under its endogenous cis-regulatory control, we find a dramatic
220 enhancement of ectopic divisions (Fig. 5G-K). Compared to *pCYCD7;1:CYCD7;1-YFP* in which ~24%
221 of stomata were four-celled at 5 dag, in *pFAMA:CYCD7;1-YFP*, that number was ~70%, with 2% of
222 stomata being 8-celled (N=237). The amount of four-celled stomata increases to 87% at 12 dag, with
223 another 2% being 8-celled (N=153). (Fig. 5K). Quantification of fluorescence intensity indicates that
224 expression with *FAMA* and *CYCD7* promoters yields equivalent levels of CYCD7;1-YFP in GMCs (Fig
225 S1B), however, this fusion protein persists in ectopically divided GCs when expressed under the *FAMA*
226 promoter (Fig. 5L). This directly links the activity of *FAMA* as a lineage specific transcription factor
227 with the cell cycle regulator CYCD7;1 to ensure “one and only one division” to create a pair of guard
228 cells.

229

230 **Discussion**

231 We have shown that CYCD7;1 is specifically expressed in GMCs prior to the last symmetric cell
232 division that forms the 2-celled stomatal complex. Depletion of *CYCD7;1* slows down this cell division
233 whereas ectopic expression of CYCD7;1 can trigger cell divisions in GCs. Mutation of the RBR1
234 binding motif in CYCD7;1 disrupts its interaction with RBR1 and renders CYCD7;1^{LGK} incapable of
235 driving ectopic division. The connection to RBR1 fits with previous work showing that CYCD7;1
236 interacts with CDKA;1 (Van Leene et al., 2010), together supporting a role for CYCD7;1 in the
237 canonical regulatory complex for G1/S transitions and the commitment to divide. CYCD7;1 activity in
238 cell cycles, however, is directly repressed by the lineage specific transcription factor *FAMA* to ensure a
239 coupling between the cell division which terminates the stomatal lineage, and the formation of
240 terminally fated GCs. This interconnection represents a direct link between cell cycle regulators and
241 developmental decisions (Fig. 6).

242

243 CYCDs are critical for the G1/S transition and commitment to divide, and are therefore interesting
244 candidate hubs for the integration of developmental control with the cell cycle machinery. In
245 *Arabidopsis*, there are 10 D-type cyclins, some active in multiple tissues (CYCD3s, CYCD4s,
246 CYCD2;1) but others whose activity is linked to specific cell types (CYCD6;1 and CYCD7;1) or cell
247 cycle behaviors (CYCD5;1 endoreplication) (Dewitte et al., 2007; Kono et al., 2007; Sanz et al., 2011;

248 Sterken et al., 2012) (Adrian et al., 2015; Sozzani et al., 2010), this study). Phylogenetic analyses
249 showed that CYCD6;1 and CYCD7;1 proteins diverge from other D-type cyclins in *Arabidopsis* (Wang
250 et al., 2004), but also that CYCD7;1 most closely resembles the single D-type cyclin in *Physcomitrella*
251 (Menges et al., 2007), consistent with our observation that it could promote G1/S transitions (a core
252 D-type activity) in multiple cell types.

253

254 Interestingly, both CYCD6;1 and CYCD7;1 are limiting for essential formative divisions during
255 development. In the root, CYCD6;1 is important for the cortex endodermis initial daughter (CEID) cell
256 divisions (Sozzani et al., 2010; Weimer et al., 2012). Here, SHORTROOT (SHR) directly activates
257 expression of CYCD6;1 which works in concert with CDKA;1 to trigger the formative division of the
258 CEID (Cruz-Ramírez et al., 2012; Sozzani et al., 2010; Weimer et al., 2012). This interaction promotes
259 the initiation of an asymmetric stem-cell division program. In contrast, CYCD7;1 expression marks the
260 boundary between two types of divisions: the continual asymmetric divisions of meristemoids vs. the
261 single symmetric division of a GMC. Here we find a quantitative requirement for *MUTE* to promote full
262 CYCD7;1 expression, but a clear requirement for FAMA and FLP/MYB88 to repress CYCD7;1 after
263 GMC division. The low expression level of CYCD7;1 in the absence of *MUTE* may point to a direct role
264 for *MUTE* in activating CYCD7;1 expression. *MUTE* is structurally similar to FAMA, and therefore
265 might be able to interact with *CYCD7;1* regulatory sequences. Alternatively, as meristemoid cells in
266 *mute* never transition into GMCs, low *CYCD7;1* levels may be an indirect consequence of altered cell
267 fate. In either case, it is notable that the introduction of CYCD7;1-YFP in *mute* did drive not additional
268 meristemoid cell divisions suggesting that CYCD7;1's division-promoting behavior requires a threshold
269 level not reached in this genetic background.

270

271 It is tempting to speculate that spatiotemporal restriction of CYCDs could be a mechanism to control the
272 cell cycle machinery more efficiently and to cope with different developmental programs. The
273 importance of these specialized CYCDs, however, must be squared with the relatively minor phenotypes
274 associated with their loss—neither *CYCD7;1* nor *CYCD6;1* mutants abolish the production of
275 specialized cells or tissue layers (Fig. 2) (Sozzani et al., 2010)). Most likely, CYCD6;1 and CYCD7;1
276 assist other, more general, cyclins in executing the cell division programs or ensure particularly high cell
277 cycle kinase activity. In the case of the stomatal lineage, CYCD3;1 and CYCD3;2, despite being
278 considered general G1/S cyclins (Dewitte et al., 2007; Dewitte et al., 2003; Menges et al., 2006), also

279 show high expression in the stomatal lineage (Adrian et al., 2015). It is also important to recognize that
280 CYCD/CDKA complexes likely have many downstream targets and that increased kinase activity could
281 induce different downstream processes, either in a feedback loop or for differentiation processes. In
282 plants, specific CDK/cyclin complexes can have differential activity towards individual substrates, and
283 both CDK and cyclin proteins contribute to substrate recognition (Harashima and Schnittger, 2012),
284 however, there is evidence that between the CDK and cyclin, the cyclin may have a more prominent role
285 (Weimer et al., 2016). Specific expression of individual cyclins, such as CYCD7;1 in the stomatal
286 lineage, therefore, could contribute to fine-tuning of cell division control and downstream substrate
287 recognition.

288

289 Leaves lose overall division competency as they mature, leading to a situation where GMCs are
290 surrounded by post-mitotic cells. Formation of functional stomata, however, requires a cell division to
291 produce two cells, suggesting that this division has unique additional regulation. Stomata are found in
292 remarkably diverse patterns and exhibit a 10-fold variation in size in different species (McElwain et al.,
293 2016), yet there have still to be reports of more than two stomatal guard cells flanking a pore. Therefore,
294 despite the ease with which we could create four-celled stomata through experimental manipulation, in
295 nature, regulation to ensure a single division appears crucial.

296 **Material and Methods**

297 **Plant material and growth conditions**

298 *Arabidopsis thaliana* Columbia-0 (Col-0) was used as wild type in all experiments. All mutants and
299 transgenic lines tested have this ecotype background. Seedlings were grown on half-strength Murashige
300 and Skoog (MS) medium (Caisson labs, USA) medium at 22°C under 16 hour-light/8 hour-dark cycles
301 and were examined at the indicated time. The following previously described mutants and reporter lines
302 were used in this study: *mute* (Pillitteri et al., 2007); *fama-1* (Ohashi-Ito and Bergmann, 2006);
303 *fhp;myb88* (Lai et al., 2005); *proSPCH:SPCH:CFP* and *proMUTE:MUTE-YFP* (Davies and Bergmann,
304 2014); *proRBR1:RBR1-CFP* (Cruz-Ramírez et al., 2012), *pro35S:CDKB1;1-N161* (Boudolf et al.,
305 2004); *proCDKB1;1:GUS* (Boudolf et al., 2004).

306

307 ***CYCD7;1* mutants**

308 *CYCD7;1* mutants FLAG_369E02 (*cyclin D1-1*) and FLAG_498H08 (*cyclin D1-2*) were derived from the
309 INRA/Versaille collection (Versaille, France) and *cyclin D1;1* was backcrossed twice to Col-0.
310 GK_496G06-019628 was derived from the GABI-Kat collection (Cologne, Germany). SALK_068423
311 and SALK_068526 were obtained from ABRC (Columbus, USA).

312

313 **Vector construction and plant transformation**

314 Constructs were generated using the Gateway® system (Invitrogen, CA, USA). Appropriate genome
315 sequences (PCR amplified from Col-0 or from entry clones) were cloned into Gateway compatible entry
316 vectors, typically pENTR/D-TOPO (Life Technologies, CA, USA), to facilitate subsequent cloning into
317 plant binary vectors pHGY (Kubo et al., 2005) or R4pGWB destination vector system (Nakagawa et al.,
318 2008; Tanaka et al., 2011). The translational reporter for CYCD7;1 was generated by cloning the
319 genomic fragment (promoter+CDS) into the entry vector pENTR to generate the entry vector CYCD7;1-
320 genomic-pENTR, followed by LR recombination into the destination vector pHGY to generate the final
321 construct. For the translational reporter for CYCD7;1^{LGK}, the LxCxE motif of CYCD7;1-genomic-
322 pENTR was mutated to LxGxK by site directed mutagenesis using the QuikChange II Kit (Agilent, CA,
323 USA) to generate the entry clone CYCD7;1-genomic-pENTR and then recombined into pHGY. The
324 transcriptional reporters for CYCD7;1 were generated by cloning the CYCD7;1 promoter region into
325 pENTR, then recombined into the destination vectors pHGY (cytosolic YFP). The other constructs
326 generated in this study *proCYCD7;1:YFP-YFPnls*, *proFAMA:FAMA-CFP*, *proML1:CYCD7;1-YFP*,

327 *proML1:CYCD7;1*, *proCYCD7;1:CYCD7;1*, and *proFAMA:CYCD7;1-YFP* were generated with the
328 tripartite recombination of the plant binary vector series R4pGWB (Nakagawa et al., 2008; Tanaka et
329 al., 2011), with the Gateway entry clones of the promoters and coding sequences compatible with the
330 binary R4pGWB destination vector system. Primer sequences used for entry clones are provided in
331 Table 1. Transgenic plants were generated by Agrobacterium-mediated transformation (Clough, 2005)
332 and transgenic seedlings were selected by growth on half-strength MS plates supplemented with 50
333 mg/L Hygromycin (pHGY, p35HGY, pGWB1, pGWB540 based constructs) or Kanamycin 100 mg/L
334 (pGWB440 and pGWV401 based constructs) or 12 mg/L of Basta (pGWB640 based constructs).

335

336 **Confocal and DIC microscopy**

337 For confocal microscopy, images were taken with a Leica SP5 microscope and processed in ImageJ.
338 Cell outlines were visualized by either 0.1 mg/ml propidium iodide in water (Molecular Probes, OR,
339 USA) incubation for 10 min, rinsed in H₂O once). For DIC microscopy, samples were cleared in 7:1
340 ethanol:acetic acid, treated 30 min with 1N potassium hydroxide, rinsed in water, and mounted in
341 Hoyer's medium. Differential contrast interference (DIC) images were obtained from the middle region
342 of adaxial epidermis of cotyledons on a Leica DM2500 microscope or Leica DM6 B microscope.

343

344 **Quantification of fluorescent intensity**

345 Images of GMCs in cotyledons were taken at 4 dag with identical settings and processed in ImageJ.
346 Fluorescent intensity was measured as mean gray value in the nucleus, subtracted by the background.
347 Measurements were averaged for mutant and control experiments with Student's-t-test used to determine
348 the statistical significance.

349

350 **GUS staining**

351 5-day old seedlings were incubated in staining solution for 12 hours and destained in 70% ethanol at 60–
352 70°C for four hours. Staining solution for 5ml: 100µl of 10% Triton X-100, 250µl 1M NaPO₄ (pH 7.2),
353 100µl 100mM potassium ferrocyanide, 100µl potassium ferricyanide, 400µl 25 mM X-Gluc, 4050µl
354 dH₂O. Images were taken with a Leica DM6 B microscope.

355

356

357

358 **EdU labeling**

359 EdU labeling was performed using the Click-iT® EdU Alexa Fluor® 488 Imaging Kit (ThermoFisher
360 Scientific, MA, USA). 4-day old seedlings were incubated in 20µM EdU solution in half-strength MS
361 for 90 minutes at room temperature. Seedlings were transferred to new tubes and washed three times
362 with wash buffer (1% BSA in PBS). Wash buffer was removed and fixation buffer was added (3.7%
363 formaldehyde in PBS) for 30 min at room temperature. Seedlings were transferred to new tubes and
364 washed two times with permeabilization buffer (0.5% Triton x-100 in PBS) for 10 minutes each,
365 protected from light on a slow rocking platform. Plants were transferred to new tubes and incubated in
366 reaction cocktail (455µL Click-IT reaction buffer, 20µL CuSO₄, 2µL Alexa Fluor Azide 488, 25 µL 1x
367 Click-IT EdU additive) for 1 hour at room temperature, protected from light, without agitation.
368 Seedlings were transferred to new tubes and washed twice for 10 minutes at room temperature with
369 wash buffer on a slow rocking platforms, protected from light. Cotyledons were imaged using a Leica
370 SP5 microscope not more than two hours after the completion of washes and processed in ImageJ.
371

372 **qPCR**

373 100 mg ground frozen material from 8-day old plants was used for RNA extraction according to the
374 manufacturer's manual (RNeasy Mini Kit, Qiagen, Germany). 1µg total RNA was used as a template for
375 cDNA synthesis (iScript cDNA synthesis kit, BioRad, CA, USA). qPCR setup was according to the
376 manual of the SsoAdvanced Universal SYBR Green Supermix (BioRad, CA, USA). qPCR was
377 performed by CFX96 Real Time C1000 Thermal Cycler (BioRad, CA, USA) according to the following
378 reaction conditions: 95°C for 30 s, followed by 39 cycles at 95°C for 10 s and at 60°C for 30 s. ACTIN
379 was used as a reference gene for all qPCRs performed. Primers can be found in Table 1.
380

381 **Table 1: Primers used in this study.**

	Forward primer (5'-3')	Reverse primer
CYCD7 genomic region (promoter + CDS)	CACCGAGAACTATAGTAGAAGGAAAC	AATGTAATTGACATTCAATTG
CYCD7;1 ^{LGK} genomic	TAATCTACTCGGAGAAAATCTGGCCCGCGAGTCC	CTCGGGGCCAAGATTTCTCGAGTAG ATTATCC
CYCD7;1 promoter	CACCGAGAACTATAGTAGAAGGAAAC	GCGGCCGTTGAAACTGAACCGGTTT
CYCD7;1 genomic	CACCATGGATAATCTACTCTGCGAAG	AATGTAATTGACATTCAATTG
CYCD7;1 ^{LGK} genomic	CACCATGGATAATCTACTCTGCGAAG	AATGTAATTGACATTCAATTG
CYCD7;1 qPCR	TCCATGCGTTCAATGGCTAATCC	TCCACCATCCAATTGTCCATTG
ACTIN qPCR	CAAGGCCGAGTATG	GAAACGCAGACGTA
<i>cycl</i> 7;1-1 RB T-DNA	CCAGACTGAATGCCACAGGCCGTC	

CYCD7;1	ATGGATAATCTACTCTGCGA	AATGTAATTTGACATTCAATTG
---------	----------------------	------------------------

382

383

384 **Acknowledgments**

385 We thank members of the Bergmann lab for helpful comments on the manuscript and Charles Hachez
386 (UCLouvain) for his contributions to the initiation of the CYCD7;1 project.

387

388

389 **Competing Interests**

390 The authors declare no competing or financial interest.

391 **Funding**

392 AKW is supported by a postdoctoral fellowship from the German Research Foundation (DFG). DCB is
393 an investigator of the Howard Hughes Medical Institute.

394 **References**

395 **Adrian, J., Chang, J., Ballenger, C. E., Bargmann, B. O. R., Alassimone, J., Davies, K. A., Lau, O.**
396 **S., Matos, J. L., Hachez, C., Lanctot, A., et al.** (2015). Transcriptome dynamics of the stomatal
397 lineage: birth, amplification, and termination of a self-renewing population. *Dev. Cell* **33**, 107–118.

398 **Borghi, L., Gutzat, R., Fütterer, J., Laizet, Y., Hennig, L. and Gruissem, W.** (2010). Arabidopsis
399 **RETINOBLASTOMA-RELATED** is required for stem cell maintenance, cell differentiation, and
400 lateral organ production. *Plant Cell* **22**, 1792–1811.

401 **Boudolf, V., Barrôco, R., Engler, J. de A., Verkest, A., Beeckman, T., Naudts, M., Inzé, D. and De**
402 **Veylder, L.** (2004). B1-type cyclin-dependent kinases are essential for the formation of stomatal
403 complexes in *Arabidopsis thaliana*. *Plant Cell* **16**, 945–955.

404 **Bramsiepe, J., Wester, K., Weinl, C., Roodbarkelari, F., Kasili, R., Larkin, J. C., Hülskamp, M.**
405 **and Schnittger, A.** (2010). Endoreplication controls cell fate maintenance. *PLoS Genet.* **6**,
406 e1000996.

407 **Clough, S. J.** (2005). Floral dip: agrobacterium-mediated germ line transformation. *Methods Mol. Biol.*
408 **286**, 91–102.

409 **Collins, C., Dewitte, W. and Murray, J. A. H.** (2012). D-type cyclins control cell division and
410 developmental rate during *Arabidopsis* seed development. *J. Exp. Bot.* **63**, 3571–3586.

411 **Cruz-Ramírez, A., Díaz-Triviño, S., Blilou, I., Grieneisen, V. A., Sozzani, R., Zamioudis, C.,**
412 **Miskolczi, P., Nieuwland, J., Benjamins, R., Dhonukshe, P., et al.** (2012). A bistable circuit
413 involving SCARECROW-RETINOBLASTOMA integrates cues to inform asymmetric stem cell
414 division. *Cell* **150**, 1002–1015.

415 **Davies, K. A. and Bergmann, D. C.** (2014). Functional specialization of stomatal bHLHs through
416 modification of DNA-binding and phosphoregulation potential. *PNAS* **111**, 15585–15590.

417 **De Veylder, L., Beeckman, T. and Inzé, D.** (2007). The ins and outs of the plant cell cycle. *Nat. Rev.*
418 *Mol. Cell Biol.* **8**, 655–665.

419 **Desvoyes, B., Ramirez-Parra, E., Xie, Q., Chua, N.-H. and Gutierrez, C.** (2006). Cell Type-Specific
420 Role of the Retinoblastoma/E2F Pathway during *Arabidopsis* Leaf Development. *Plant Physiol.*
421 **140**, 67–80.

422 **Dewitte, W., Riou-Khamlich, C., Scofield, S., Healy, J. M. S., Jacqmard, A., Kilby, N. J. and**
423 **Murray, J. A. H.** (2003). Altered cell cycle distribution, hyperplasia, and inhibited differentiation in
424 *Arabidopsis* caused by the D-type cyclin CYCD3. *The Plant Cell* **15**, 79–92.

425 **Dewitte, W., Scofield, S., Alcasabas, A. A., Maughan, S. C., Menges, M., Braun, N., Collins, C.,**
426 **Nieuwland, J., Prinsen, E., Sundaresan, V., et al.** (2007). *Arabidopsis* CYCD3 D-type cyclins
427 link cell proliferation and endocycles and are rate-limiting for cytokinin responses. *PNAS* **104**,
428 14537–14542.

429 **Friedman, W. E.** (1999). Expression of the cell cycle in sperm of *Arabidopsis*: implications for

430 understanding patterns of gametogenesis and fertilization in plants and other eukaryotes.
431 *Development* **126**, 1065–1075.

432 **Gutzat, R., Borghi, L. and Gruissem, W.** (2012). Emerging roles of RETINOBLASTOMA-
433 RELATED proteins in evolution and plant development. *Trends Plant Sci.* **17**, 139–148.

434 **Harashima, H. and Schnittger, A.** (2012). Robust reconstitution of active cell-cycle control complexes
435 from co-expressed proteins in bacteria. *Plant Methods* **8**, 23.

436 **Harashima, H., Dissmeyer, N. and Schnittger, A.** (2013). Cell cycle control across the eukaryotic
437 kingdom. *Trends in Cell Biology* **23**, 345–356.

438 **Harbour, J. W. and Dean, D. C.** (2000). The Rb/E2F pathway: expanding roles and emerging
439 paradigms. *Genes Dev.* **14**, 2393–2409.

440 **Inzé, D. and De Veylder, L.** (2006). Cell cycle regulation in plant development. *Annu. Rev. Genet.* **40**,
441 77–105.

442 **Kanaoka, M. M., Pillitteri, L. J., Fujii, H., Yoshida, Y., Bogenschutz, N. L., Takabayashi, J., Zhu,
443 J.-K. and Torii, K. U.** (2008). SCREAM/ICE1 and SCREAM2 specify three cell-state transitional
444 steps leading to arabidopsis stomatal differentiation. *Plant Cell* **20**, 1775–1785.

445 **Katagiri, Y., Hasegawa, J., Fujikura, U., Hoshino, R., Matsunaga, S. and Tsukaya, H.** (2016). The
446 coordination of ploidy and cell size differs between cell layers in leaves. *Development* **143**, 1120–
447 1125.

448 **Kono, A., Umeda-Hara, C., Adachi, S., Nagata, N., Konomi, M., Nakagawa, T., Uchimiya, H. and
449 Umeda, M.** (2007). The Arabidopsis D-type cyclin CYCD4 controls cell division in the stomatal
450 lineage of the hypocotyl epidermis. *Plant Cell* **19**, 1265–1277.

451 **Kubo, M., Udagawa, M., Nishikubo, N., Horiguchi, G., Yamaguchi, M., Ito, J., Mimura, T.,
452 Fukuda, H. and Demura, T.** (2005). Transcription switches for protoxylem and metaxylem vessel
453 formation. *Genes Dev.* **19**, 1855–1860.

454 **Lai, L. B., Nadeau, J. A., Lucas, J., Lee, E.-K., Nakagawa, T., Zhao, L., Geisler, M. and Sack, F. D.**
455 (2005). The Arabidopsis R2R3 MYB proteins FOUR LIPS and MYB88 restrict divisions late in the
456 stomatal cell lineage. *Plant Cell* **17**, 2754–2767.

457 **Lau, O. S. and Bergmann, D. C.** (2015). MOBE-ChIP: a large-scale chromatin immunoprecipitation
458 assay for cell type-specific studies. *Plant J.* **84**, 443–450.

459 **Lau, O. S., Davies, K. A., Chang, J., Adrian, J., Rowe, M. H., Ballenger, C. E. and Bergmann, D.**
460 (2014). Direct roles of SPEECHLESS in the specification of stomatal self-renewing cells.
461 *Science* **345**, 1605–1609.

462 **Lee, E., Liu, X., Egli, Y. and Sack, F.** (2013). FOUR LIPS and MYB88 conditionally restrict the G1/S
463 transition during stomatal formation. *J. Exp. Bot.* **64**, 5207–5219.

464 **MacAlister, C. A., Ohashi-Ito, K. and Bergmann, D. C.** (2007). Transcription factor control of
465 asymmetric cell divisions that establish the stomatal lineage. *Nature* **445**, 537–540.

466 **Matos, J. L. and Bergmann, D. C.** (2014). Convergence of stem cell behaviors and genetic regulation
467 between animals and plants: insights from the *Arabidopsis thaliana* stomatal lineage. *F1000Prime*
468 *Rep* **6**, 53.

469 **Matos, J. L., Lau, O. S., Hachez, C., Cruz-Ramírez, A., Scheres, B. and Bergmann, D. C.** (2014).
470 Irreversible fate commitment in the *Arabidopsis* stomatal lineage requires a FAMA and
471 RETINOBLASTOMA-RELATED module. *Elife* **3**, 1792.

472 **McElwain, J. C., Yiotis, C. and Lawson, T.** (2016). Using modern plant trait relationships between
473 observed and theoretical maximum stomatal conductance and vein density to examine patterns of
474 plant macroevolution. *New Phytologist* **209**, 94–103.

475 **Menges, M., Hennig, L., Gruisse, W. and Murray, J. A. H.** (2003). Genome-wide gene expression
476 in an *Arabidopsis* cell suspension. *Plant Mol. Biol.* **53**, 423–442.

477 **Menges, M., Pavesi, G., Morandini, P., Bögre, L. and Murray, J. A. H.** (2007). Genomic
478 organization and evolutionary conservation of plant D-type cyclins. *Plant Physiol.* **145**, 1558–1576.

479 **Menges, M., Samland, A. K., Planchais, S. and Murray, J. A. H.** (2006). The D-type cyclin
480 CYCD3;1 is limiting for the G1-to-S-phase transition in *Arabidopsis*. *The Plant Cell* **18**, 893–906.

481 **Nakagami, H., Kawamura, K., Sugisaka, K., Sekine, M. and Shinmyo, A.** (2002). Phosphorylation
482 of retinoblastoma-related protein by the cyclin D/cyclin-dependent kinase complex is activated at
483 the G1/S-phase transition in tobacco. *The Plant Cell* **14**, 1847–1857.

484 **Nakagawa, T., Nakamura, S., Tanaka, K., Kawamukai, M., Suzuki, T., Nakamura, K., Kimura, T.**
485 **and Ishiguro, S.** (2008). Development of R4 Gateway Binary Vectors (R4pGWB) Enabling High-
486 Throughput Promoter Swapping for Plant Research. *Bioscience, Biotechnology, and Biochemistry*
487 **72**, 624–629.

488 **Nowack, M. K., Harashima, H., Dissmeyer, N., Zhao, X., Bouyer, D., Weimer, A. K., De Winter,**
489 **F., Yang, F. and Schnittger, A.** (2012). Genetic framework of cyclin-dependent kinase function in
490 *Arabidopsis*. *Dev. Cell* **22**, 1030–1040.

491 **Ohashi-Ito, K. and Bergmann, D. C.** (2006). *Arabidopsis* FAMA controls the final
492 proliferation/differentiation switch during stomatal development. *Plant Cell* **18**, 2493–2505.

493 **Pillitteri, L. J. and Torii, K. U.** (2007). Breaking the silence: three bHLH proteins direct cell-fate
494 decisions during stomatal development. *BioEssays* **29**, 861–870.

495 **Pillitteri, L. J., Sloan, D. B., Bogenschutz, N. L. and Torii, K. U.** (2007). Termination of asymmetric
496 cell division and differentiation of stomata. *Nature* **445**, 501–505.

497 **Riou-Khamlich, C., Menges, M., Healy, J. M. S. and Murray, J. A. H.** (2000). Sugar Control of the
498 Plant Cell Cycle: Differential Regulation of *Arabidopsis* D-Type Cyclin Gene Expression. *Mol.*

499 *Cell. Biol.* **20**, 4513–4521.

500 **Roeder, A. H. K., Chickarmane, V., Cunha, A., Obara, B., Manjunath, B. S. and Meyerowitz, E.**
501 M. (2010). Variability in the control of cell division underlies sepal epidermal patterning in
502 *Arabidopsis thaliana*. *PLoS Biol.* **8**, e1000367.

503 **Sanz, L., Dewitte, W., Forzani, C., Patell, F., Nieuwland, J., Wen, B., Quelhas, P., De Jager, S.,**
504 **Titmus, C., Campilho, A., et al.** (2011). The *Arabidopsis* D-Type Cyclin CYCD2;1 and the
505 Inhibitor ICK2/KRP2 Modulate Auxin-Induced Lateral Root Formation. *The Plant Cell* **23**, 641–
506 660.

507 **Schellmann, S., Schnittger, A., Kirik, V., Wada, T., Okada, K., Beermann, A., Thumfahrt, J.,**
508 **Jürgens, G. and Hülskamp, M.** (2002). TRPTYCHON and CAPRICE mediate lateral inhibition
509 during trichome and root hair patterning in *Arabidopsis*. *The EMBO Journal* **21**, 5036–5046.

510 **Sozzani, R., Cui, H., Moreno-Risueno, M. A., Busch, W., Van Norman, J. M., Vernoux, T., Brady,**
511 **S. M., Dewitte, W., Murray, J. A. H. and Benfey, P. N.** (2010). Spatiotemporal regulation of cell-
512 cycle genes by SHORTROOT links patterning and growth. *Nature* **466**, 128–132.

513 **Sterken, R., Kiekens, R., Boruc, J., Zhang, F., Vercauteren, A., Vercauteren, I., De Smet, L.,**
514 **Dhondt, S., Inzé, D., De Veylder, L., et al.** (2012). Combined linkage and association mapping
515 reveals CYCD5;1 as a quantitative trait gene for endoreduplication in *Arabidopsis*. *PNAS* **109**,
516 4678–4683.

517 **Tanaka, Y., Nakamura, S., Kawamukai, M., Koizumi, N. and Nakagawa, T.** (2011). Development
518 of a series of gateway binary vectors possessing a tunicamycin resistance gene as a marker for the
519 transformation of *Arabidopsis thaliana*. *Bioscience, Biotechnology, and Biochemistry* **75**, 804–807.

520 **Uemukai, K., Iwakawa, H., Kosugi, S., de Uemukai, S., Kato, K., Kondorosi, E., Murray, J. A., Ito,**
521 **M., Shinmyo, A. and Sekine, M.** (2005). Transcriptional activation of tobacco E2F is repressed by
522 co-transfection with the retinoblastoma-related protein: cyclin D expression overcomes this
523 repressor activity. *Plant Mol. Biol.* **57**, 83–100.

524 **Umen, J. G. and Goodenough, U. W.** (2001). Control of cell division by a retinoblastoma protein
525 homolog in Chlamydomonas. *Genes Dev.* **15**, 1652–1661.

526 **Van Leene, J., Hollunder, J., Eeckhout, D., Persiau, G., Van De Slijke, E., Stals, H., Van Isterdael,**
527 **G., Verkest, A., Neirynck, S., Buffel, Y., et al.** (2010). Targeted interactomics reveals a complex
528 core cell cycle machinery in *Arabidopsis thaliana*. *Molecular Systems Biology* **6**, 397.

529 **Vandepoele, K., Raes, J., De Veylder, L., Rouzé, P., Rombauts, S. and Inzé, D.** (2002). Genome-
530 Wide Analysis of Core Cell Cycle Genes in *Arabidopsis*. *The Plant Cell* **14**, 903–916.

531 **Vanneste, S., Coppens, F., Lee, E., Donner, T. J., Xie, Z., Van Isterdael, G., Dhondt, S., De Winter,**
532 **F., De Rybel, B., Vuylsteke, M., et al.** (2011). Developmental regulation of CYCA2s contributes to
533 tissue-specific proliferation in *Arabidopsis*. *The EMBO Journal* **30**, 3430–3441.

534 **Wang, G., Kong, H., Sun, Y., Zhang, X., Zhang, W., Altman, N., DePamphilis, C. W. and Ma, H.**

535 (2004). Genome-wide analysis of the cyclin family in Arabidopsis and comparative phylogenetic
536 analysis of plant cyclin-like proteins. *Plant Physiol.* **135**, 1084–1099.

537 **Weimer, A. K., Biedermann, S., Harashima, H., Roodbarkelari, F., Takahashi, N., Foreman, J.,**
538 **Guan, Y., Pochon, G., Heese, M., Van Damme, D., et al.** (2016). The plant-specific CDKB1-
539 CYCB1 complex mediates homologous recombination repair in Arabidopsis. *The EMBO Journal*
540 **35**, 2068–2086.

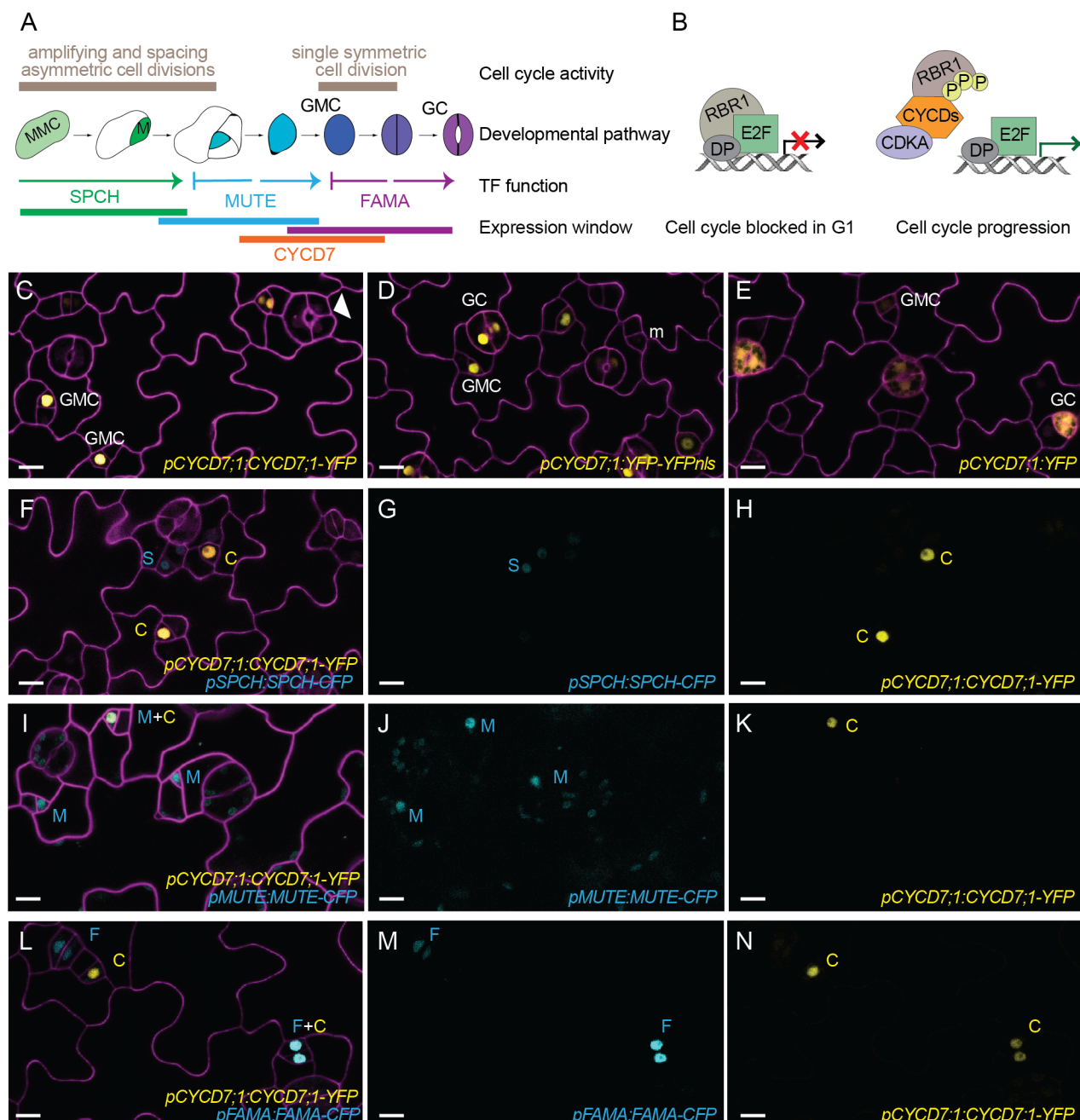
541 **Weimer, A. K., Nowack, M. K., Bouyer, D., Zhao, X., Harashima, H., Naseer, S., De Winter, F.,**
542 **Dissmeyer, N., Geldner, N. and Schnittger, A.** (2012). Retinoblastoma related1 regulates
543 asymmetric cell divisions in Arabidopsis. *Plant Cell* **24**, 4083–4095.

544 **Xie, Z., Lee, E., Lucas, J. R., Morohashi, K., Li, D., Murray, J. A. H., Sack, F. D. and Grotewold,**
545 **E.** (2010). Regulation of cell proliferation in the stomatal lineage by the Arabidopsis MYB FOUR
546 LIPS via direct targeting of core cell cycle genes. *Plant Cell* **22**, 2306–2321.

547 **Zhao, X., Harashima, H., Dissmeyer, N., Pusch, S., Weimer, A. K., Bramsiepe, J., Bouyer, D.,**
548 **Rademacher, S., Nowack, M. K., Novak, B., et al.** (2012). A general G1/S-phase cell-cycle
549 control module in the flowering plant Arabidopsis thaliana. *PLoS Genet.* **8**, e1002847.

550

Figures and Figure legends

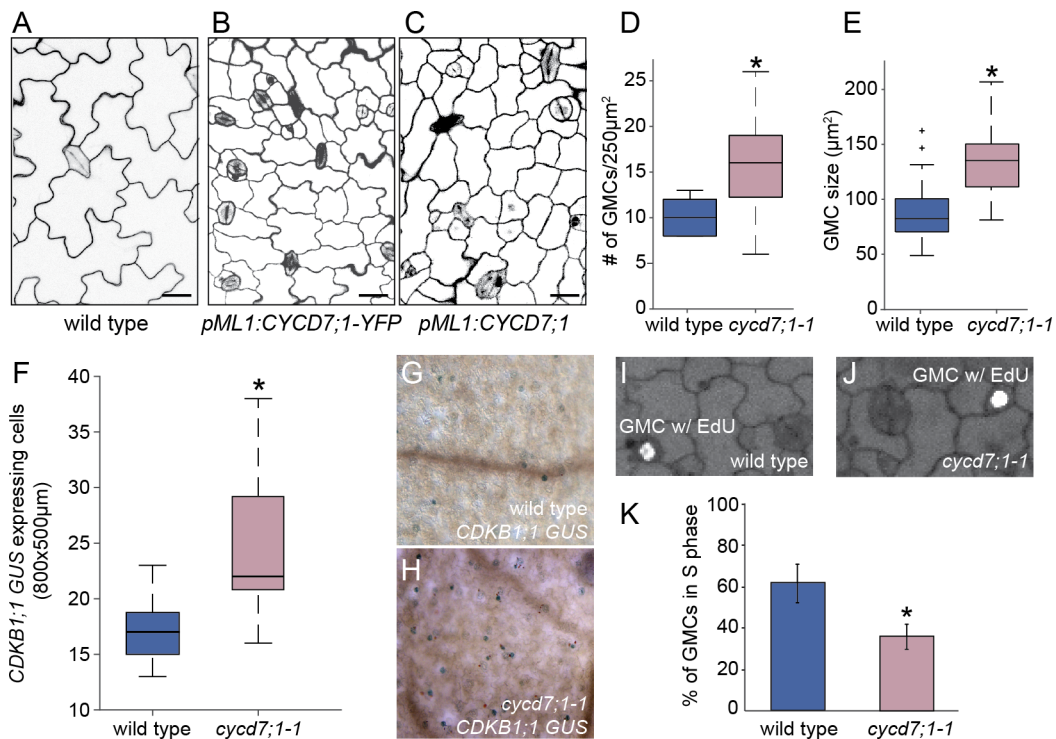


551

552 **Figure 1: CYCD7;1 is expressed in GMCs prior to the last symmetric division of the stomatal
553 lineage**

554 **(A)** Scheme of stomatal development in *Arabidopsis thaliana*. Cell cycle activity depicted in beige, with
555 cell fate transitions, function and expression window of master bHLH transcription factors SPCH
556 (green), MUTE (blue), and FAMA (purple) and CYCD7;1 (orange). Meristemoid mother cells (light

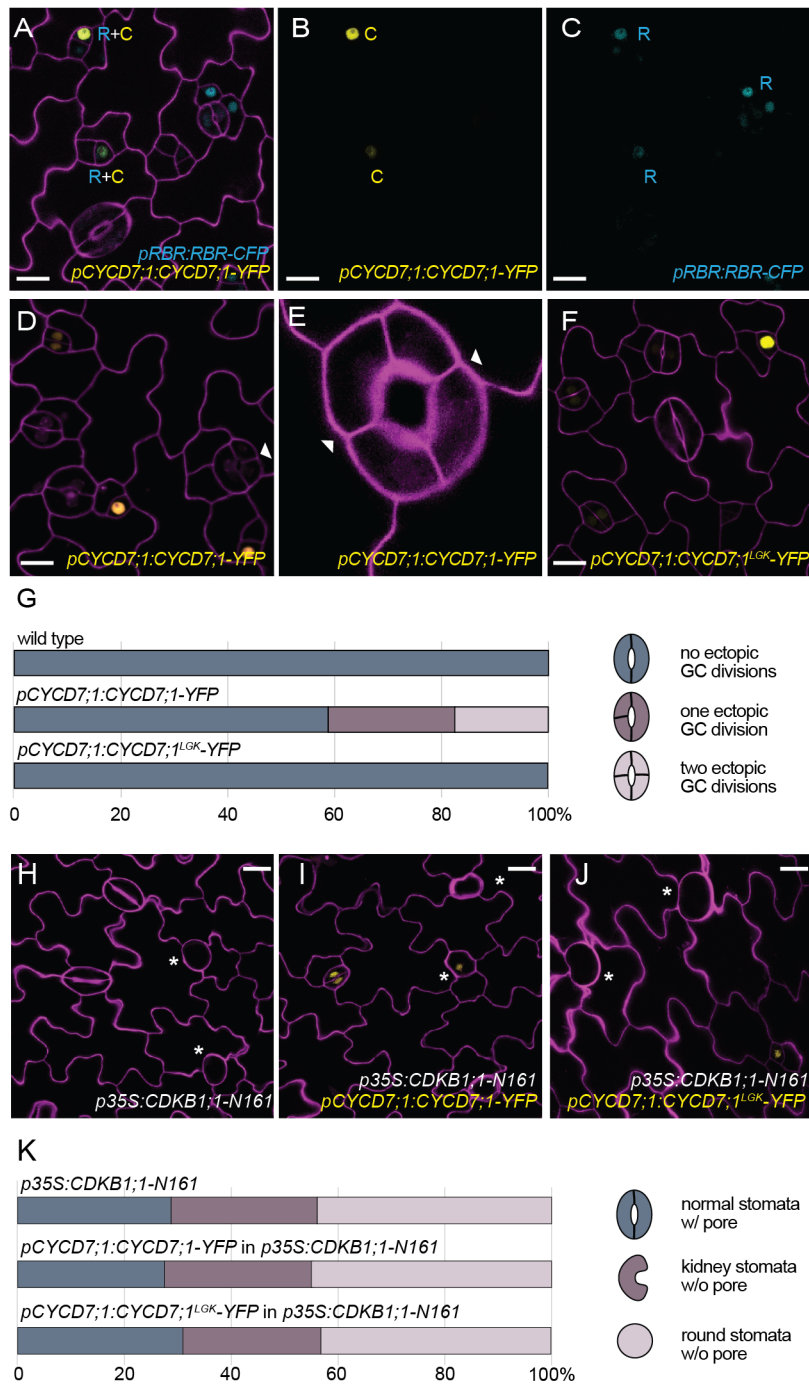
557 green, MMC) divide asymmetrically to enter the lineage. Meristemoids (green) can undergo amplifying
558 and spacing asymmetric cell divisions until activity is terminated. Guard mother cells (GMC, blue)
559 reenter the cell cycle only once to generate the pair of symmetric guard cells (GC, purple). **(B)** Cartoon
560 of plant RBR1/CYCD complexes driving the G1 to S transition and commitment to divide. RBR1 binds
561 to E2F-DP transcription factors and blocks their ability to induce transcription of S phase genes. CYCDs
562 interact with RBR1 through their LxCxE motif and facilitate phosphorylation of RBR1 by the
563 CDKA;1/CYCD complex. Upon phosphorylation RBR1 releases E2F transcription factors, which leads
564 to expression of S phase genes for DNA replication. **(C-E)** Expression of the translational reporter
565 *pCYCD7;1:CYCD7;1-YFP*, the transcriptional reporters *pCYCD7;1:YFP-YFPnls* and *pCYCD7;1:YFP*
566 (all yellow) in abaxial cotyledons. White arrowheads point at ectopic cell divisions. **(F-N)** Co-
567 expression of *pCYCD7;1:CYCD7;1-YFP* (yellow, C) and *pSPCH:SPCH-CFP* (cyan, S),
568 *pMUTE:MUTE-CFP* (cyan, M) and *pFAMA:FAMA-CFP* (cyan, F).
569
570 Confocal images were taken at 5 dag (days after germination). Cell outlines (magenta) are visualized
571 with propidium iodide. All images are at the same magnification and scale bar is 10 μ M.



572

573 **Figure 2: CYCD7;1 promotes cell divisions**

574 (A-C) Confocal images of adaxial cotyledon epidermes of wild type, and plant expressing
575 *pML1:CYCD7;1-YFP* and *pML1:CYCD7;1* at 6 dag. Cell outlines were visualized with propidium
576 iodide (magenta). Scale bar 20 μM . (D) Quantification of the number of GMCs in wild type and *cyclin D1-1*
577 cotyledons at 4 dag. Asterisk indicates significant difference (p-value = 0.0032; Mann-Whitney U
578 test). (E) Quantification of GMC area in wild type (N=55) and *cyclin D1-1* (N=51) cotyledons at 4 dag.
579 Asterisk indicates significant difference (p-value = 6.76E-13; Mann-Whitney U test). (F) Quantification
580 of cells expressing the *CDKB1;1-GUS* marker in wild type and *cyclin D1-1* cotyledons at 5 dag.
581 Asterisk indicates significant difference (p-value = 0.0023; Mann-Whitney U test). (G) Image of wild type
582 cotyledon expressing *CDKB1;1-GUS* marker at 5 dag. (H) Image of *cyclin D1-1* cotyledon expressing
583 *CDKB1;1-GUS* marker at 5 dag. (I) Image of wild type GMC with EdU (5-ethynyl-2'-deoxyuridine)
584 labeling at 4 dag cotyledon. (J) Image of *cyclin D1-1* GMC with EdU labeling, 4-day old cotyledon. (K)
585 Quantification of EdU labeling in wild type and *cyclin D1-1* mutants. Graph shows the % of GMCs in S
586 phase during a 90-minute incubation with EdU. Error bars indicate the 95% confidence interval.
587 Asterisk indicates significant difference (p-value = 7x10E-6; Fisher's Exact Test).
588 Center lines in box plots show the medians; box limits indicate the 25th and 75th percentiles; whiskers
589 extend 1.5 times the interquartile range from the 25th and 75th percentiles.

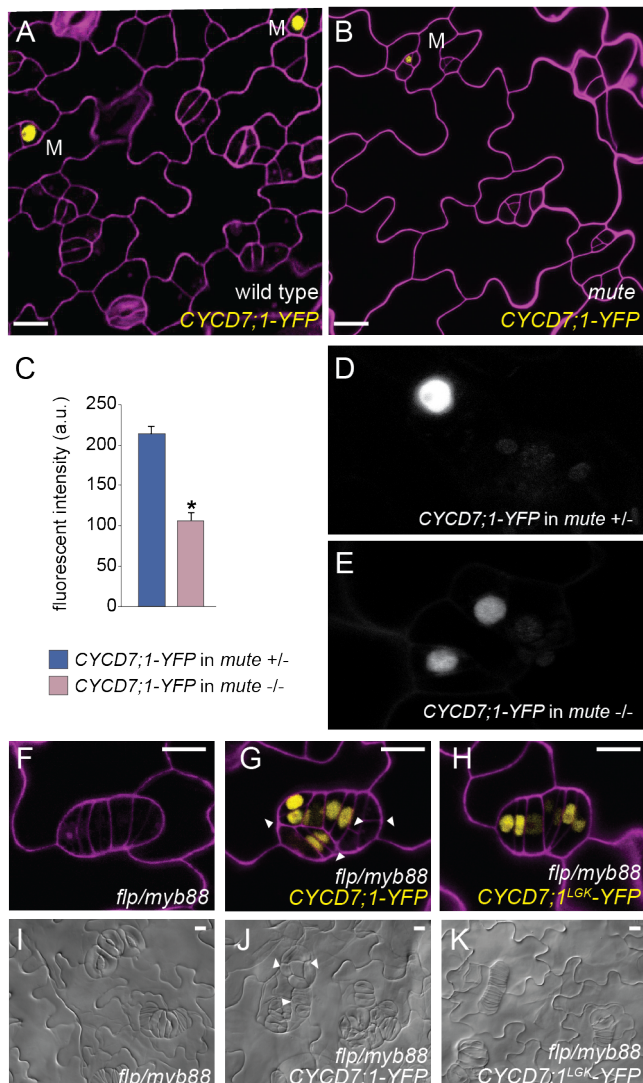


590

591 **Figure 3: CYCD7;1 requires RBR1 binding and CDKB1;1 activity for ectopic cell divisions**

592 **(A-C)** Co-expression of *pCYCD7;1:CYCD7;1-YFP* (yellow, C) and *pRBR1:RBR1-CFP* (cyan, R) in
 593 GMCs at 5 dag. **(D-E)** Expression of *pCYCD7;1:CYCD7;1-YFP* drives ectopic cell divisions (white
 594 arrowheads). **(F)** Expression of *pCYCD7;1:CYCD7;1^{LGK}-YFP* (yellow) does not drive ectopic cell
 595 divisions. **(G)** Quantification of ectopic cell divisions in GCs at 5 dag in cotyledons in wild type

596 (N=173), *pCYCD7;1:CYCD7;1-YFP* (N=306) and *pCYCD7;1:CYCD7;1^{LGK}-YFP* (N=288). **(H)**
597 Phenotype of dominant negative *p35S:CDKB1;1-N161* at 6 dag. White asterisks label arrested GMCs.
598 **(I-J)** Failure of *pCYCD7;1:CYCD7;1-YFP* (I) and *pCYCD7;1:CYCD7;1^{LGK}-YFP* (J) to suppress
599 *CDKB1;1-N161* phenotype at 6 dag. White asterisks label arrested GMCs. **(K)** Quantification of stomata
600 phenotypes in cotyledons in *p35S:CDKB1;1-N161* (N=238), *pCYCD7;1:CYCD7;1-YFP* in
601 *p35S:CDKB1;1-N161* (N=296) and *pCYCD7;1:CYCD7;1^{LGK}-YFP* in *p35S:CDKB1;1-N161* (N=217) at
602 6 dag.
603 Confocal images show cell outlines (magenta) stained with propidium iodide. Scale bar 10 μ m (A-D, F)
604 and 20 μ m (H-J).

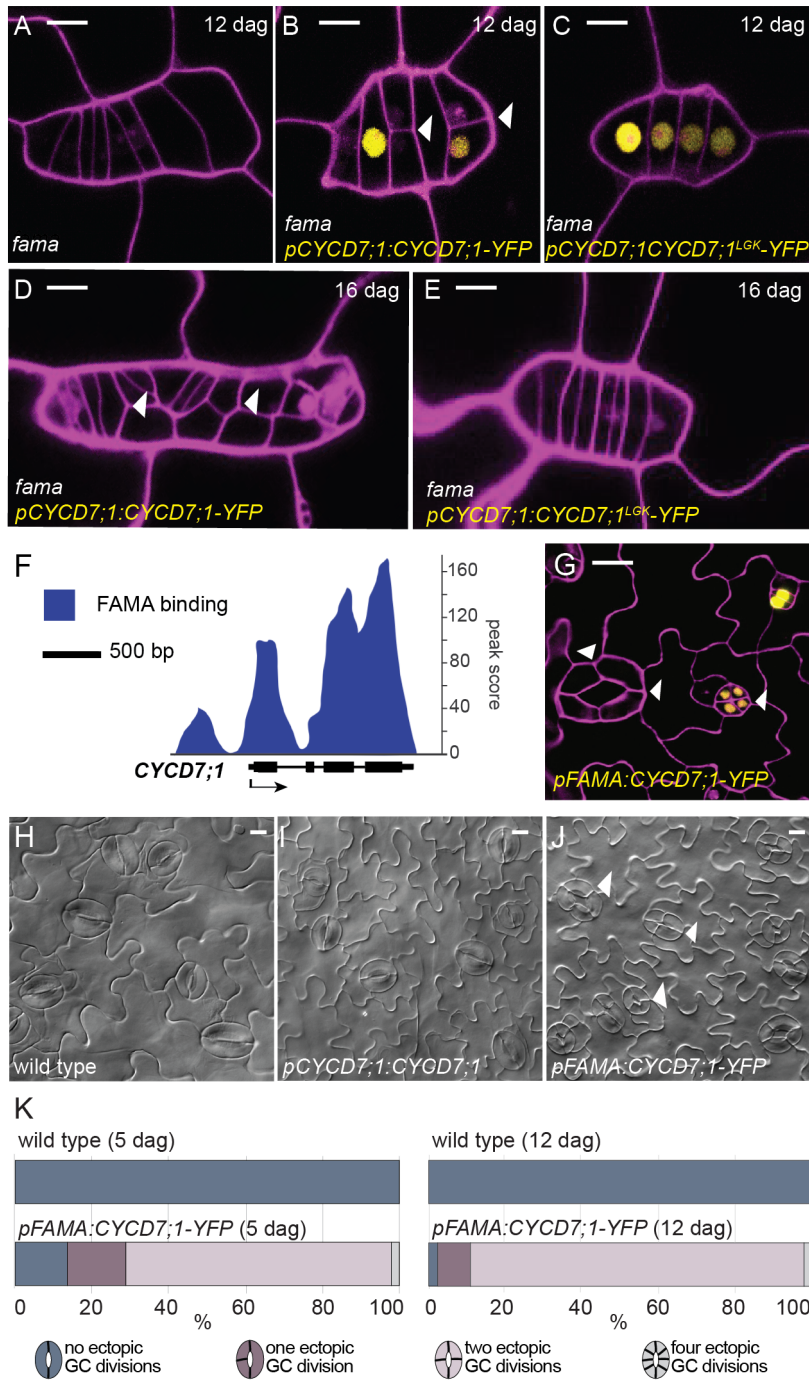


605

606 **Figure 4: CYCD7;1-YFP is expressed at low levels in *mute* mutants and persists and drives ectopic**
607 **divisions in *flp/myb88* mutants**

608 **(A, B)** Wild type and *mute* mutants expressing *pCYCD7;1:CYCD7;1-YFP* in 6 day old cotyledons. Scale
609 bar 10 μ m; M, meristemoid. **(C-E)** Quantification of fluorescence intensity of *CYCD7;1-YFP* in
610 homozygous *mute* mutants (N=27) and their heterozygous or wild-type sister plants (N=21) (a.u.,
611 arbitrary units). Images of cotyledons were taken at 4 dag. Error bars show standard error. Asterisk
612 shows statistical significance (p-value <0.0001; Student-t test). **(F)** Phenotype of the double mutant
613 *flp/myb88* at 6 dag. **(G)** Expression of *pCYCD7;1:CYCD7;1-YFP* in *flp/myb88* drives ectopic divisions
614 in tumors at 6 dag. **(H)** Expression of *pCYCD7;1:CYCD7;1^{LGK}-YFP* in *flp/myb88* is less able to drive
615 ectopic divisions at 6 dag. **(I)** DIC images of the phenotype of the double mutant *flp/myb88* at 12 dag.
616 **(J)** Expression of *pCYCD7;1:CYCD7;1-YFP* in *flp/myb88* drives ectopic divisions in tumors at 12 dag.

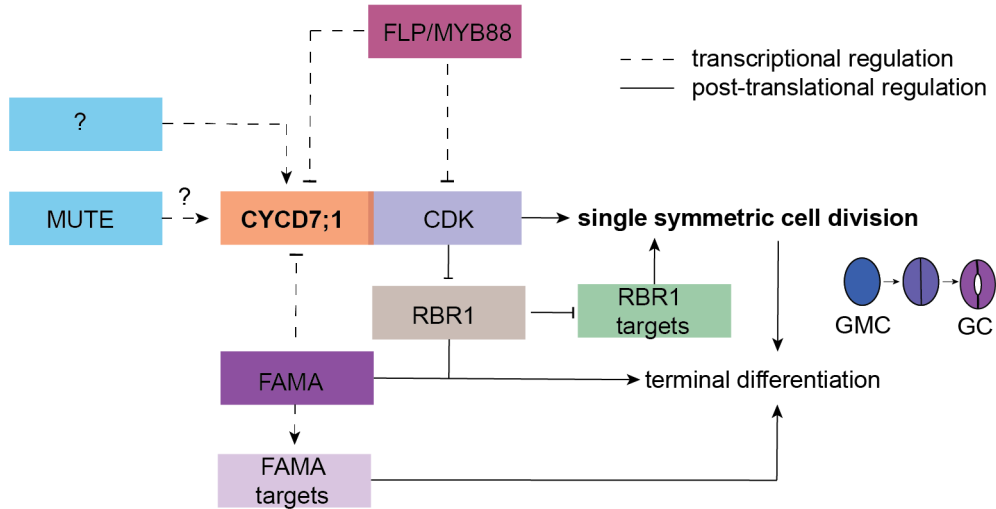
617 (K) Expression of *pCYCD7;1:CYCD7;1^{LGK}-YFP* in *flp/myb88* is less able to drive ectopic divisions at
618 12 dag. White arrowheads label ectopic divisions. Confocal images show cell outlines (magenta) stained
619 with propidium iodide. Scale bar 10 μ M.



620

621 **Figure 5: CYCD7;1 expression is regulated by FAMA which serves to constrain CYCD7;1 activity**
622 **(A-E)** Confocal images of *fama*, *pCYCD7;1:CYCD7;1-YFP* in *fama* mutant background and
623 *pCYCD7;1:CYCD7;1^{LGK}-YFP* in *fama* mutant background at 12 or 16 dag, respectively. **(F)** ChIP-Seq
624 profile of FAMA binding to the promoter and gene body of *CYCD7;1*. Black arrow indicates gene
625 orientation and transcriptional start sites. **(G)** Confocal image of *pFAMA:CYCD7;1-YFP* at 5 dag. White

626 arrowheads show ectopic division and prolonged CYCD7;1-YFP presence. **(H-J)** DIC images of abaxial
627 cotyledon epidermis of wild type, *pCYCD7;1:CYCD7;1* and *pFAMA:CYCD7;1-YFP* at 12 dag. Scale
628 bar, 10 μ M. Arrowheads point at ectopic cell divisions. **(K)** Quantification of ectopic cell divisions in
629 wild type (N=142) and *pFAMA:CYCD7;1-YFP* (N=237) at 5 dag and in wild type (N=125) and
630 *pFAMA:CYCD7;1-YFP* (N=153) at 12 dag. Confocal images show cell outlines (magenta) stained with
631 propidium iodide. Scale bar 10 μ m.

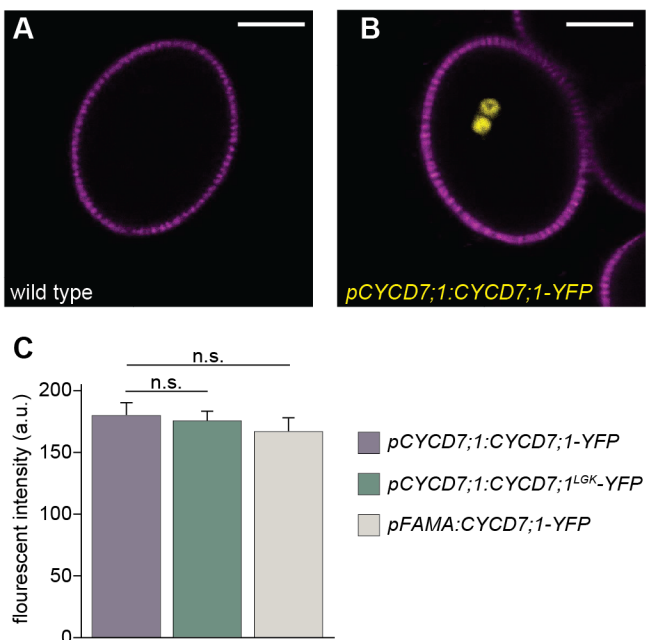


632

633 **Figure 6: Model of the developmental integration of CYCD7;1 to ensure lineage specific cell cycle**
634 **regulation**

635 Cell cycle regulators are integrated with stomatal specific transcriptions factors to ensure the last
636 formative division of the lineage that creates one pair of symmetric guard cells. Initiation of CYCD7;1's
637 expression in GMCs requires factors in addition to MUTE (question mark). CYCD7;1 together with its
638 CDK partner executes the formative division of the GMC. Due to the observation that this last division
639 is not completely abolished in *cycl7;1* mutants, other D-type cyclins likely back up G1-S phase
640 transition. CDK/CYCD complexes phosphorylate RBR1 in order to release its negative function on S
641 phase promoting factors. To ensure termination of the lineage, the transcription factor FAMA, itself
642 slightly later expressed than CYCD7;1, binds to the CYCD7;1 promoter to temporally control
643 expression of the lineage-specific CYCD7;1 to GMCs and to restrict the cell cycle right after the last
644 division. Transcriptional regulation is marked by dashed lines. This regulatory network ensures high cell
645 cycle activity for the last formative division in the stomatal lineage and terminates cell division activity
646 to "one and only one" division.

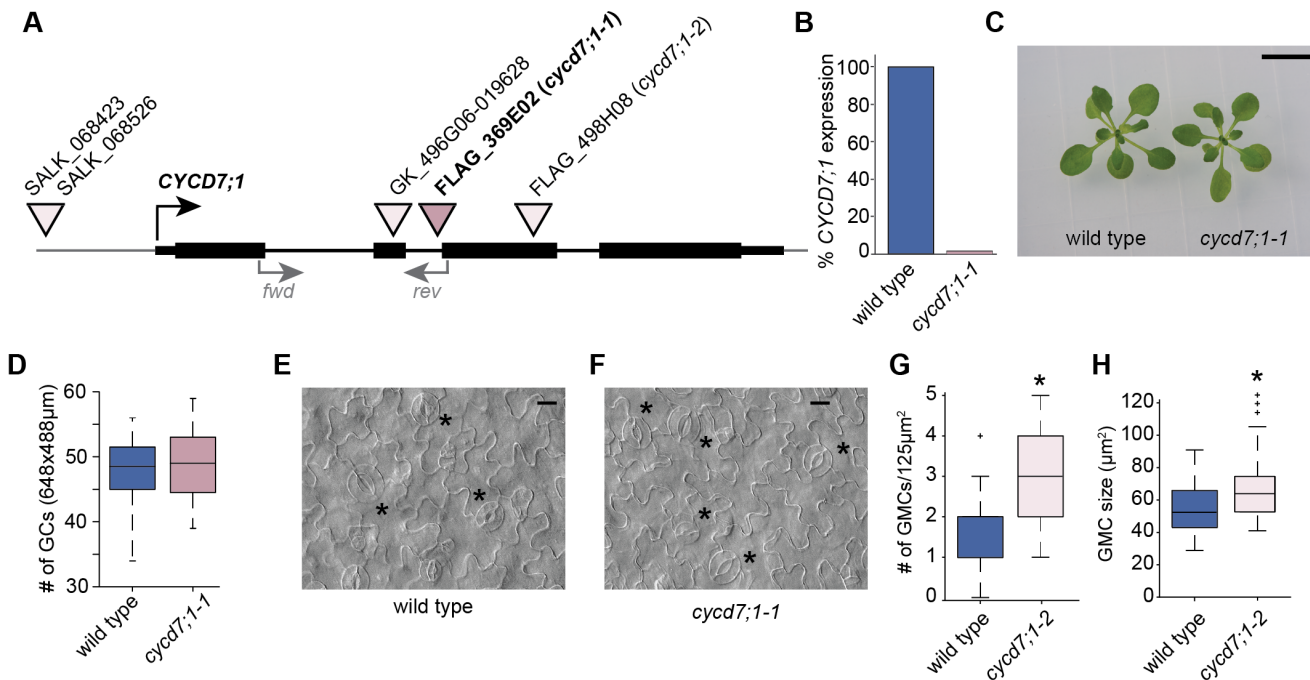
647 **Supplementary Figures**



648

649 **Figure S1: CYCD7;1 expression patterns**

650 **(A, B)** CYCD7;1 (yellow) is expressed in sperm cells during pollen anthesis. **(C)** Intensity
651 measurements of fluorescent nuclei were 179 a.u. +/-10 SE for *proCYCD7;1:CYCD7;1-YFP* vs 176 a.u.
652 +/-8 SE for *proCYCD7;1:CYCD7;1^{LGK}-YFP* (N=15 nuclei/line; p> 0.05; Student's t-test) and
653 *proCYCD7;1:CYCD7;1-YFP* 166 a.u. +/-11 SE for *proFAMA:CYCD7;1-YFP* (N=15 nuclei/line; p>
654 0.05; Student's t-test). Error bars show standard error. a.u., arbitrary units; n.s. non-significant; SE,
655 standard error.



656

657 **Figure S2: T-DNA insertion lines and phenotype of *cycd7;1* mutants**

658 (A) Schematic drawing of *CYCD7;1* gene structure with available T-DNA insertion lines and their
 659 insertion sites. Black boxes indicate exons. Gray arrowheads marked with *fwd* and *rev* show primer
 660 binding sites for qPCR. (B) qPCR of *CYCD7;1* expression in wild type and the *cycd7;1-1* mutant.
 661 Primer binding sites are shown in (A). (C) Wild type and *cycd7;1-1* mutant seedlings at 14 dag. (D)
 662 Quantification of GCs in wild type and *cycd7;1-1* mutants at 5 dag on the abaxial side of cotyledons (N
 663 =12 cotyledons for each genotype). Difference between the wild type and *cycd7;1-1* is not significant (p-
 664 value = 0.8169; Mann-Whitney U test). (E) Wild type cotyledon with mature GCs, labeled with black
 665 asterisks at 7 dag. (F) Cotyledon of *cycd7;1-1* mutant with mature GCs, labeled with black asterisks,
 666 images were taken at 7 dag. (G) Quantification of the number of GMCs in wild type and *cycd7;1-2*
 667 cotyledons at 4 dag. Asterisk indicates significant difference (p-value = 0.0031; Mann-Whitney U test).
 668 (H) Quantification of GMC area in wild type (N=29) and *cycd7;1-2* (N=46) cotyledons, 4 dag. Asterisk
 669 indicates significant difference (p-value = 0.0053; Mann-Whitney U test).
 670 Center lines show the medians; box limits indicate the 25th and 75th percentiles; whiskers extend 2.5
 671 times the interquartile range from the 97.5th percentile. Scale bar 1 cm in (C) and 20 μ M in (E and F).